Supporting Information

Structural Transitions in Nanoparticle Assemblies Governed by Competing Nanoscale Forces

Rachelle Choueiri, [†] Anna Klinkova,[†] Heloise Thérien-Aubin,[†] Michael Rubinstein,[*,*]
Eugenia Kumacheva[†,‡, §,*]

[†]Department of Chemistry, University of Toronto, 80 Saint George Street, Toronto, Ontario M5S 3H6, Canada
[‡]Department of Chemical Engineering and Applied Chemistry, University of Toronto, 200 College Street, Toronto, Ontario M5S 3E5, Canada
[*] Department of Chemistry, University of North Carolina, Chapel Hill, North Carolina 27599-3290, USA
[§]The Institute of Biomaterials and Biomedical Engineering, University of Toronto, 4 Taddle Creek Road, Toronto, Ontario M5S 3G9, Canada

Synthesis of gold nanoparticles

Cetyltrimethylammonium bromide (CTAB)-coated gold nanoparticles (NPs) were synthesized according to a two-step seed-mediated procedure reported elsewhere.[1] Briefly, a seed solution was prepared by the reducing $HAuCl_4$ (10 mL, 5×10^{-4} M) in 10 mL of citrate aqueous solution (5×10^{-4} M) by using the addition of ice-cold solution of $NaBH_4$ in water (0.6 mL, 0.1 M) under stirring. Ten minutes after borohydride solution was added, the stirring was stopped and the solution was stored at room temperature for 2-3 h.

A solution was prepared by dissolving $HAuCl_4$ (2.5×10^{-3} M) and CTAB (0.08 M) in water. To 9 mL of this mixture, 0.5 mL of 0.1 M aqueous ascorbic acid was added. Immediately after that, 10 mL of seeds was added to the above solution under vigorous stirring. The mixture, denoted "Solution A", was stirred for 10 min and subsequently, used within 30 min after its preparation.

Another solution, denoted "Solution B", was prepared by dissolving $HAuCl_4$ (2.5×10^{-3} M) and CTAB (0.08 M) in water. To 9 mL of this mixture, 0.5 mL of 0.1 M aqueous ascorbic acid was added. Following the addition, 9 mL of "Solution A" was added under vigorous stirring. After stirring for 10 min, the NP-containing solution was incubated at room temperature overnight

Surface functionalization of gold nanoparticles with thiol-terminated polystyrene

The as-synthesized CTAB-coated NPs were centrifuged in 1.5 mL centrifugation tubes at 10620 g for 15 min at 29 °C. After removing the supernatant, 0.3 mL of NP solution was added to 4 μM solution of thiol-terminated polystyrene (PS) in tetrahydrofuran (THF). The solution was immediately sonicated for 30 min and subsequently, incubated at room temperature for 12 h. The non-attached polymer was separated by twelve centrifugation cycles (10620 g, 23 °C, 15 min). Stock solutions of PS-coated NPs in THF were dried, in order to achieve an optical density of 2, when diluted to 1 mL. The NPs were redispersed in 0.5 mL of *N*,*N* -dimethylformamide (DMF).

Characterization of PS-coated gold nanoparticles

Carbon-coated copper Transmission Electron Microscopy (TEM) grids were purchased from Electron Microscopy Sciences. A droplet of the solution of NPs was deposited onto the carbon film, left in air for 30 s and then solvent was quickly removed with a KimWipe to prevent drying of the sample solution onto the grid. The PS-coated NPs were imaged using a Hitachi H-7000 Transmission Electron Microscope (Figure S1).

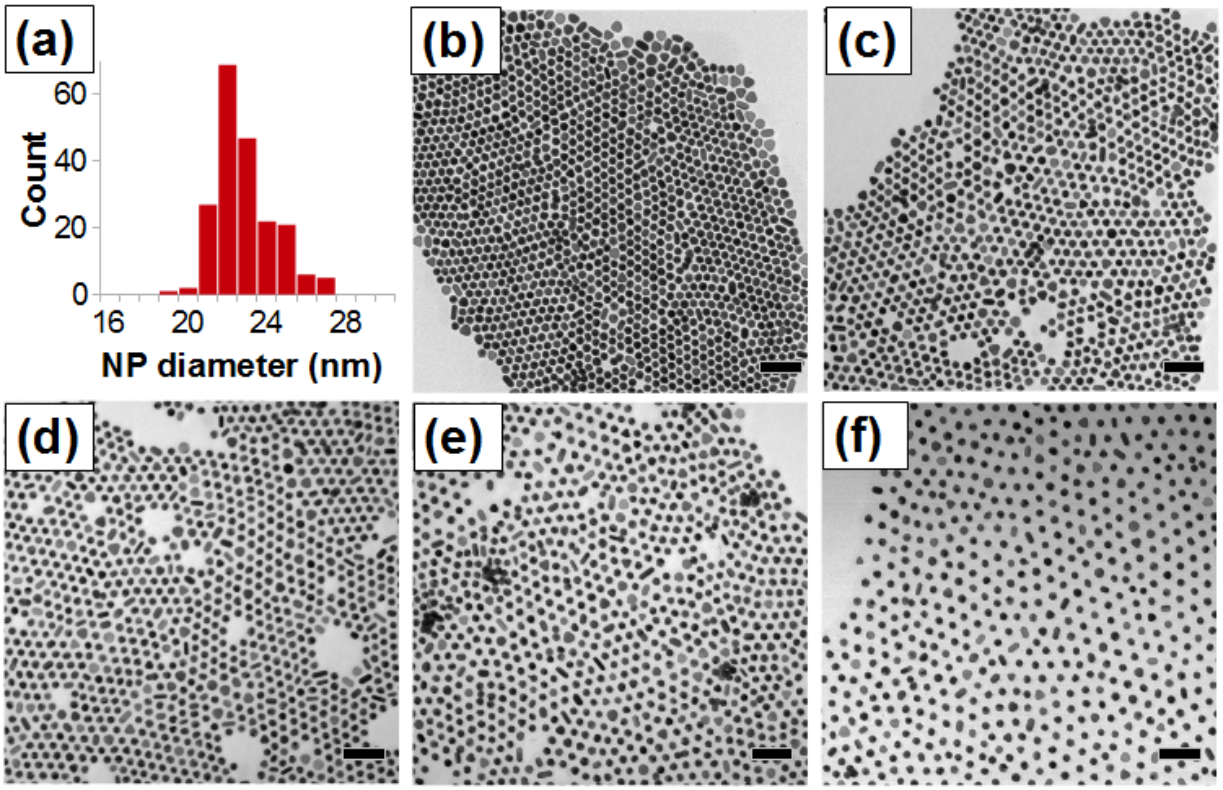

Figure S1. (a) Size distribution of gold NPs prior to ligand exchange. (b) TEM images of gold NPs deposited on the TEM grid from the solution in DMF. The NPs are stabilized with (b) PS-5K, (c) PS-12K, (d) PS-20K, (e) PS-30K and (f) PS-50K.

Dynamic light scattering and ζ-potential measurements

The distribution of NP sizes and their ζ-potentials were characterized using a Malvern Zetasizer Nano ZS instrument. The ζ-potential of the NPs was measured in the DMF/water mixture and DMF (Figure S2) at low NP concentration (O.D. ≈ 0.2), in order to prevent their aggregation during data acquisition. With increasing concentration of water, the value of ζ-potential reduced, becoming more positive, in agreement with our earlier results obtained for PS end-functionalized gold nanorods[2].

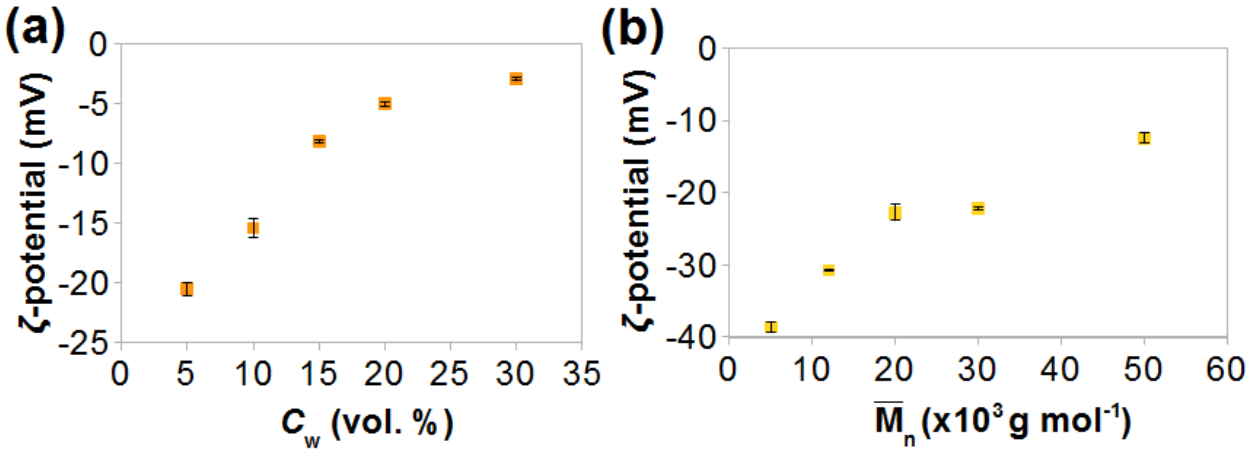

Figure S2. (a) Variation in ζ-potential for gold NPs stabilized with PS-50 K, plotted as a function of the concentration of water in the DMF-water mixture. (b) Variation in ζ-potential with polymer molecular weight in pure DMF.

Self-assembly of nanoparticles in the DMF-water mixtures

A water-DMF solution (0.5 mL) was added dropwise to 0.5 mL of the solution of NPs in DMF[3]. The concentration of water in the added DMF-water solution was tuned to achieve the final value of C_w of 2.5, 5, 7.5, 10 and 15 vol. %. After 1h or 24 h from the beginning of self-assembly, a droplet of each sample was deposited on the TEM grid and the solvent was quickly removed with a KimWipe to prevent slow drying of the sample solution onto the grid.

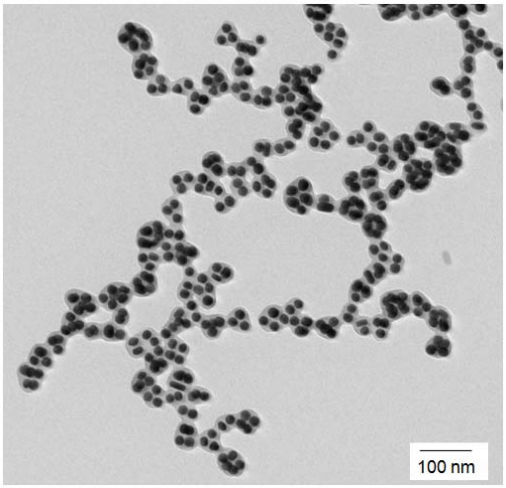

Figure S3. Networks of globules observed after 24 h for gold NPs stabilized with PS-50K at C_w = 5 vol. %.

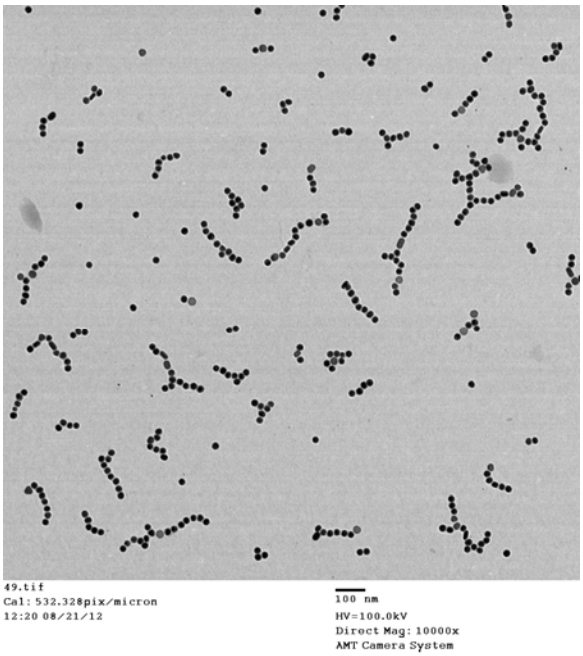

Figure S4. Chains formed from gold NPs stabilized with PS-5K at C_w = 15 vol.%. t_{SA}= 1 h.

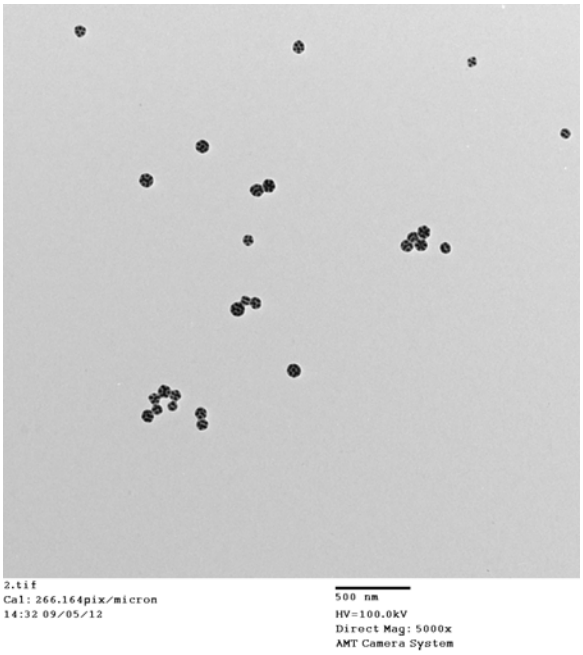

Figure S5. Globules formed by gold NPs stabilized with PS-50K at C_w = 5 vol. %. t_{SA} =1h.

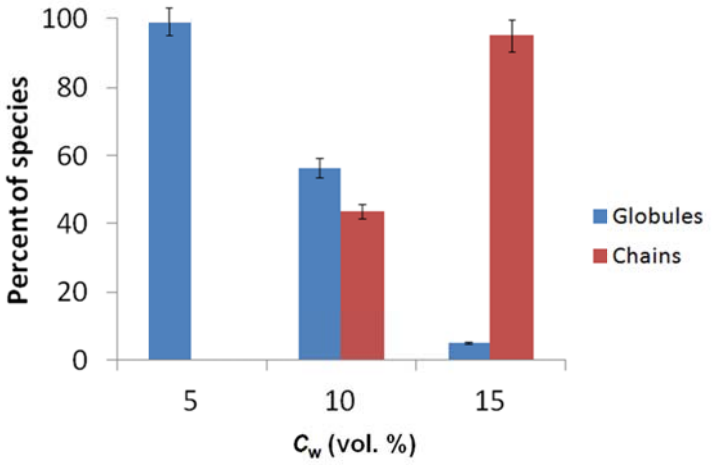

Figure S6. Fraction of population of globules and chains formed by gold NPs stabilized with PS-50K at C_w of 5, 10 and 15 vol. %. t_{SA} =1h.

Encapsulation of self-assembled structures in a diblock copolymer shell

Following work by Yang et al.,[4] Sánchez-Iglesias et al.,[5] and Grzelczak et al.,[6] we encapsulated self-assembled NP structures with poly(styrene-*b*-acrylic acid) (PS-PAA) (the molecular weights of the PS and PAA blocks were 15 000 g/mol and 3600 g/mol, respectively). Briefly, 200 µL of 4 mg/mL PS-PAA solution in DMF was added to 1 mL of NPs after 1h of self-assembly followed by addition of a DMF/water solution to reach C_w = 35 vol. %. To initiate PS-PAA micelle formation on the self-assembled structures, the colloidal solution of self-assembled structures was heated to 40 °C for 2 h and subsequently slowly cooled to room temperature. Addition of PS-PAA stalled NP self-assembly.

The resultant encapsulated assemblies were purified in three centrifugation cycles (208000 g, 15 min, 23 °C) and imaged on plasma-cleaned TEM grids. While the NP globules remained intact, for original well-defined NP chains, we observed partial change to globular structures, as shown in Figure S7, in agreement with previously reported results.[4]

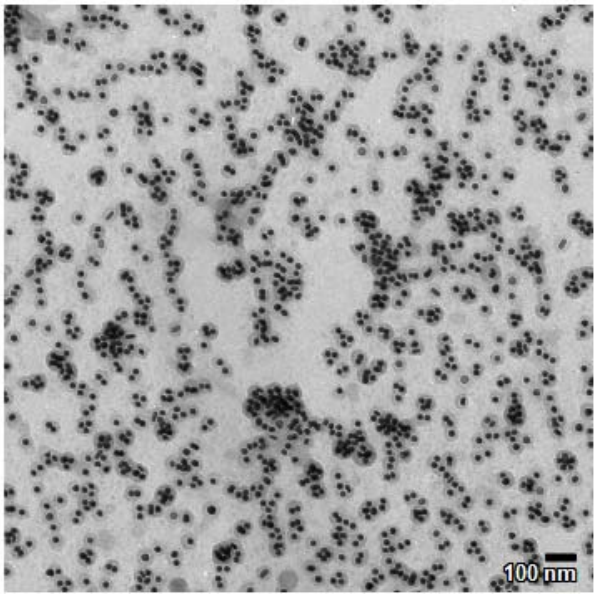

Figure S7. Representative TEM image of self-assembled structures following their encapsulation with diblock copolymer PS-PAA. The NPs were capped with 12K-PS. C_w = 60 vol. %, t_{SA} =5 min.

Self-assembly experiments conducted in the DMF/water mixture in the presence of NaCl

Self-assembly experiments in the presence of NaCl were conducted at C_w = 15 vol % and the total salt concentration of 10, 50, 100, 200 and 300 mM. To prepare solutions for self-assembly, NaCl was first, dissolved in water. The initial concentration of NaCl in water was tuned to achieve the desired concentration of the salt in the system during the self-assembly process. For example, to achieve a C_w = 15 vol. % and [NaCl]=300 mM in the self-assembly experiment, we mixed 150 μL of a 1M aqueous solution of NaCl and 350 μL of DMF and added 500 μL of this mixed solution to 500 μL of NPs suspended in DMF.

Self-assembly experiments conducted in the THF-DMF-water mixtures

Self-assembly experiments in THF-DMF/water mixtures were conducted at C_w = 15 vol. %. The ratios of volumes of THF-to-DMF were 0, 0.1, 0.5 and 1. The self-assembly was carried out similarly to the self-assembly in the DMF/water solutions.

Testing reversibility of the self-assembly experiments

To test the reversibility of structural transitions, the composition of the solvent was changed by adding a DMF/water mixture to achieve a final C_w of 1.7 vol. %, that is, conditions under which the NPs exist as individual entities. For both globules and chains, an addition of energy (either sonication for 15 min or heating at 40 °C for 1 h) was required to supplement the solvent change to yield individual NPs (Figure S8), which did not-re-associate for at least, several days.

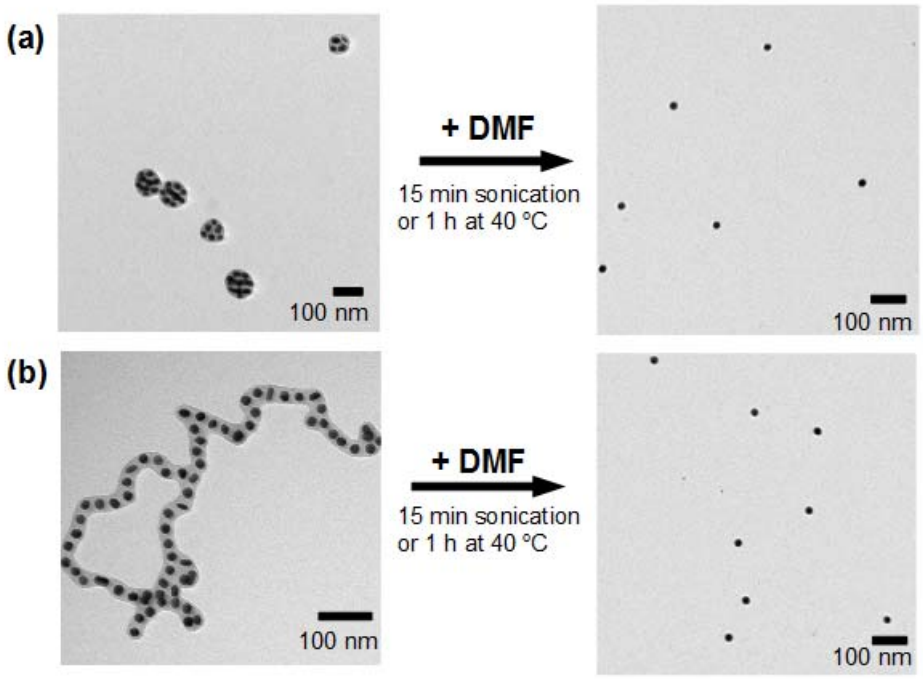

Figure S8. (a) Testing reversibility of the formation of NP globules at C_w = 5 vol. % by adding DMF to the colloidal solution of globules to achieve C_w = 1.7 vol. %. (b) Testing structural transitions of NP chains at C_w = 15 vol. % by adding a DMF to the colloidal solution of chains to achieve C_w = 1.7 vol. %. t_{SA}=1 h. The NPs were stabilized with PS-50K.

Qualitatively, the reversibility of chain-globule, as well as chain-individual NPs and globule-individual NPs transitions, has been observed in several "back-and-forth" experiments by varying the amount of water in the DMF/water mixture. Quantitatively, we found that the number of NPs per chain was larger than the number of NPs per globule. For example, in DMF/water solutions with water content of 15 and 5 vol. %, NPs stabilized with PS-50K formed chains and globules with aggregation numbers of ~30 and ~10, respectively. The difference in aggregation numbers of the chain and globular

structures originated from the different solvent quality and thus different strength of interactions between the NPs.

Testing structural transitions between globules and chains

The transition between chains and globules were tested by triggering the assembly of chain structures at C_w =15 vol. % and subsequently, reducing C_w to 5 vol. % by adding DMF to the DMF/water mixture. In agreement, with the phase diagram (Figure 2, main text), after 4 h, we observed the transformation of chains into globules, shown in Figure S9a.

In a different experiment, we induced the self-assembly of NPs in globular structures at C_w = 5 vol. % and increased C_w to 15 vol. % by adding water to the DMF/water mixture. In this case, aggregation of globules dominated over rearrangement of individual globules into chains. Figure S9b shows the formation of the network of globules. Network formation was also evidenced by the rapid assembly of flocculates in the solution and the eventual clearing of the original solution of the globules.

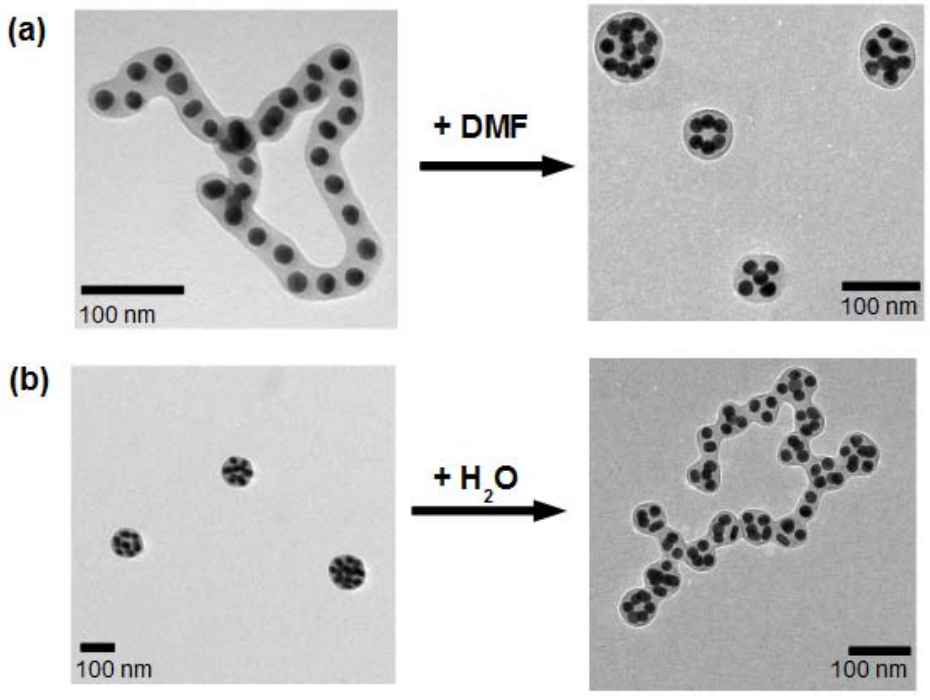

Figure S9. (a) Structural transition from NP chains (C_w = 15 vol. %) to globules (C_w = 5 vol. %), following the addition of DMF to the NP solution in the DMF/water mixture. (b) Structural transitions

from NP globules (C_w = 5 vol. %; t_{SA} = 1 h) to networks of globules (C_w = 15 vol. %). In a and b, t_{SA} = 1 h. The NPs were stabilized with PS-50K.

Determination of the interfacial tension between PS-DMF/water and DMF/water phases

Direct measurement of the interfacial tension, $\gamma_{PS/L}$, between the PS-DMF/water and DMF/water phases (denoted as "PS" and "L", respectively) was not possible, due a close-to-glassy state of the collapsed PS molecules in the DMF/water mixture. Instead, the value of $\gamma_{PS/L}$ was calculated from the individually values of surface tension of the PS-phase, γ_{PS}, and the L-phase, γ_L, by using the extended Fowkes equation[7,8] as

$$\gamma_{PS/L} = \gamma_{PS} + \gamma_L - 2\,(\gamma_{PS}^{\,d}\,\gamma_L^{\,d})^{1/2} - 2\,(\gamma_{PS}^{\,p}\,\gamma_L^{\,p})^{1/2} \qquad \text{(S1)},$$

where the superscripts *d* and *p* refer to the dispersive and polar components of the surface tension.

To determine the dispersive component of γ_L, the sessile drop method was used to measure the contact angle of the liquid on a solid substrate, which only had dispersive interactions with the liquid. The contact angle, α, was then related to the dispersive component of γ_L by using the Owens-Wendt equation as[9]

$$\gamma_L^d = \frac{\left[\gamma_L(1+\cos\alpha)\right]^2}{4\,\gamma_S^d} \qquad \text{(S2)}$$

where the γ^d_S is the dispersive component of the surface tension of the substrate used. In our work, we used poly(ethylene terephthalate) (PTFE) as the solid substrate with $\gamma_S^{\,d}$ =19.0 mN/m (the polar component of the surface tension for PTFE was zero).[10,11] The value of $\gamma_L^{\,p}$ was then found as γ_L-$\gamma_L^{\,d}$. The measured contact angles, the values of surface tension and the values for the dispersive component of the surface tension for the DMF/water solutions at C_w of 5 and 15 vol. % (the L-phase) are summarized in Table SI.

The surface tension of the PS-DMF/water mixture, γ_{PS}, was calculated to be 38.4 and 40.8 mN/m for C_w of 5 and 15 vol. %, respectively,[12,13] with polar components of 10.2 and 12.7 mN/m and

dispersive components of 28.2 and 28.1 mN/m. The values of the interfacial tension, $\gamma_{PS/L}$, calculated using eq. S1 are given in Table S1.

Table S1. Surface properties of the "PS" and "L" phases

C_w (vol. %)	γ_L (mN/m)	α (^{o})	γ_L^d (mN/m)	γ_L^p (mN/m)	γ_{PS} (mN/m)	γ_{PS}^d (mN/m)	γ_{PS}^p (mN/m)	$\gamma_{PS/L}$ (mN/m)
5	37.1	87.8	20.6	16.5	38.4	28.2	10.2	1.4
15	46.3	97.2	22.8	23.6	40.8	28.1	12.7	1.9

Calculations of the change in energy following NP assembly

Figure S10 shows schematically fragments of self-assembled nanostructures for three adjacent NPs. Based on analysis of TEM images, for the NPs functionalized with PS-50K, the radius of the gold core, R, was 11.5 nm; the total radius, R_t, of the NP with a gold core and the PS "shell" was 15.5 nm; and the center-to-center distance, D, between two adjacent NPs was 28.0 and 29.5 nm for C_w of 5 and 15 vol. %, respectively (corresponding to the thickness, d, of the PS layer confined NP surfaces of 5 and 6.5 nm, respectively). The angle θ between the lines connecting the center of the second NP with the centers of the first and the third NPs varied from 180^o (chain configuration, Figure S7a) to 60^o (globular configuration, Figure 7c). The distance, L, between the centers of the first and the third NPs changed from $4R+2d$ to $D=2R+d$ for the chain and globular configurations, respectively.

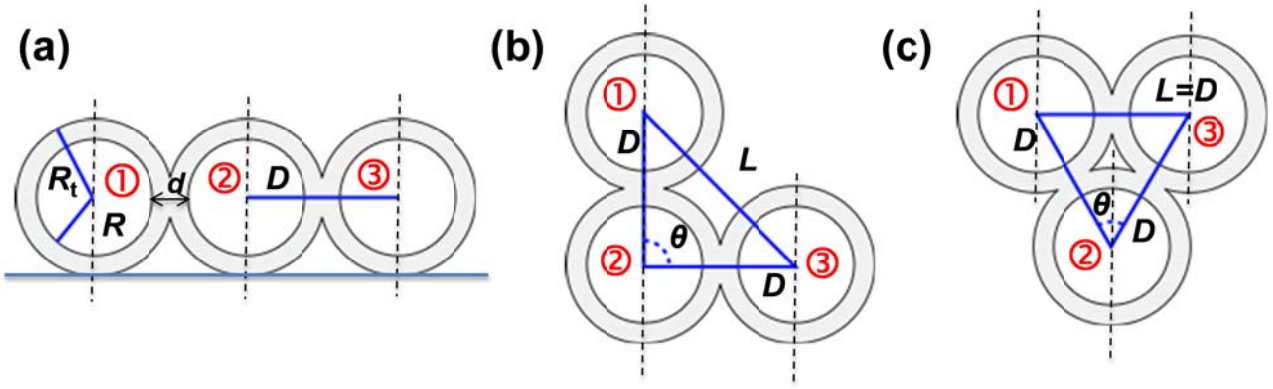

Figure S10. (a-c) Assembly of three NPs in the chain configuration (θ=180^o) (a), intermediate configuration (b) and globular configuration (θ=60 ^{o}) (c). R is the radius of the metal gold cores and R_t the radius of the particle with the PS shell.

When two NPs associated, the fragments of their surface that were originally exposed to the solvent formed contact (shown as a biconvex lens in Figure S11), thereby screening a part of PS shell from unfavorable interactions with a poor solvent and reducing the total surface energy of the system.

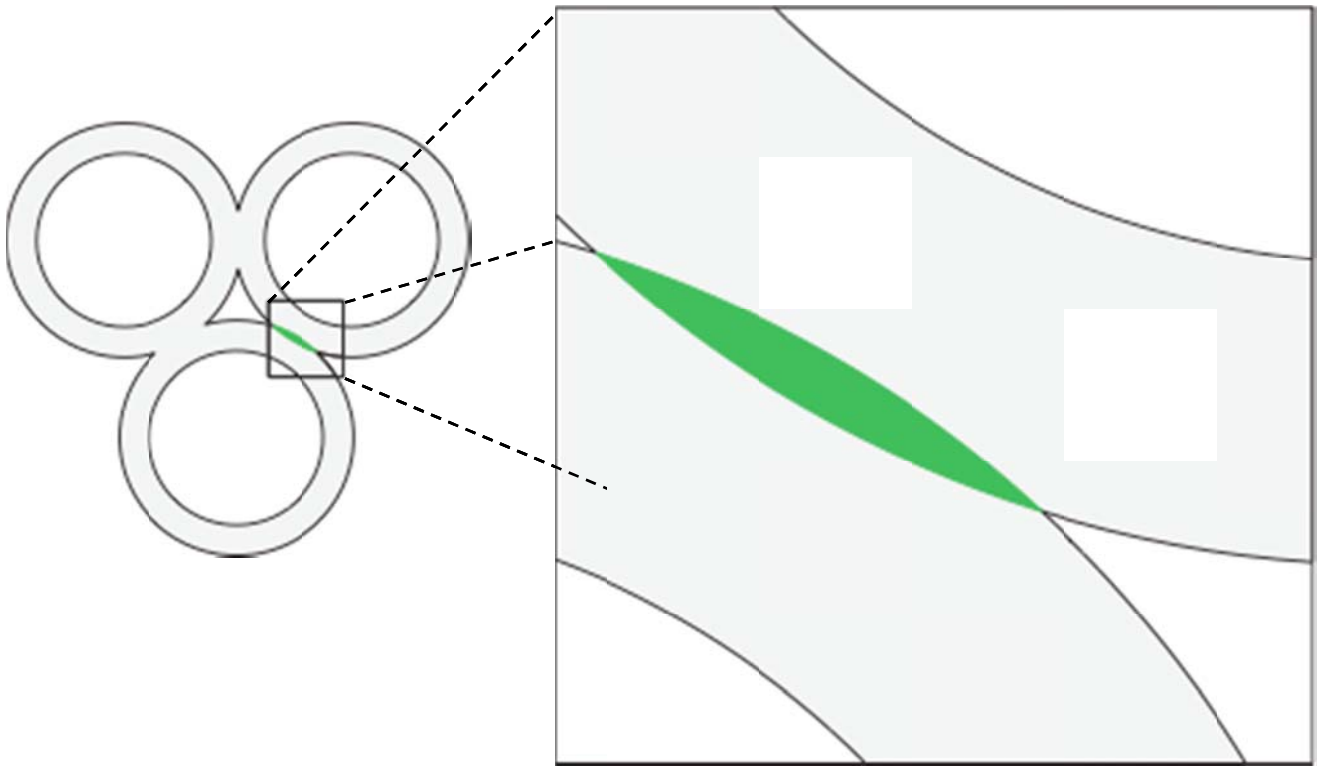

Figure S11. Schematic of the formation of the interface between two associating NPs. Overlap and adhesion of the PS shells lead to the reduction of the area of NP surface exposed to the poor solvent.

The surface area of the ensemble of two NPs exposed to poor solvent decreased as shown in Figure S11 by

$$\Delta A = -4\pi\left(R_t - \frac{L}{2}\right)R_t \quad \text{(S7)},$$

where L is given by

$$L = \sqrt{2D^2(1-\cos\theta)} \quad \text{(S8)}$$

and the notations are explained in Figure S10.

The change in attractive surface tension energy was calculated for two NPs coated with PS-50K in the DMF/water mixture at C_w of 5 and 15 vol. %, when they made a contact, with a reduction of the surface area ΔA.

$$\Delta E_{st} = \gamma_{PS/L}\,\Delta A \quad \text{(S9)}$$

The values of interfacial tension $\gamma_{PS/L}$ were 1.36×10^{-2} J/m^2 and 1.94×10^{-2} J/m^2 for the DMF/water compositions with C_w of 5 and 15 vol. %, respectively (Table S1). At large separations (or $\theta > 64^o$), the NPs did not make contact and the surface area did not change (ΔA=0), yielding ΔE_{st}=0. Red lines in Figure S12 shows that for C_w=5 vol %, the reduction in E_{st} upon contact of NPs 1 and 3 was significantly stronger than for C_w=15 vol. %.

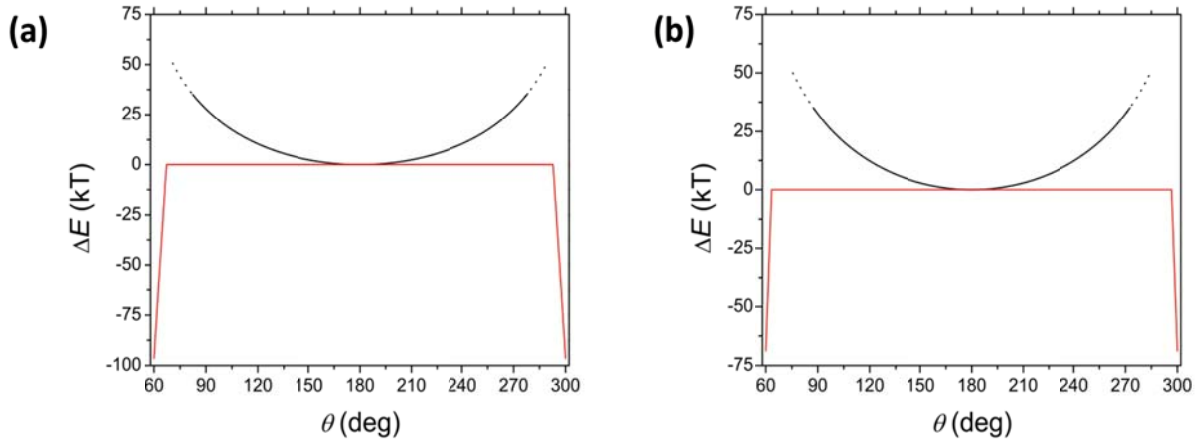

Figure S12. (a,b) Variation in surface tension energy (red lines) and electrostatic energy (black lines) between two associating NPs, when angle θ (as in Figure S10) changes from 60 to 300^o in the DMF/water solution at C_w = 5 vol. % (a) and C_w = 15 vol. % (b).

The change in electrostatic energy, ΔE_{el}, was calculated using the approximation developed for charged spherical NPs functionalized with polymer brushes[14] as a logarithmic function of the surface-to-surface interparticle distance $d=L-2R$ with respect to this distance $2D-2R$, in the chain configuration (θ=180°). By integrating the electrostatic force between particles, $F = \frac{\pi^2}{2}\frac{kT}{l_B d}R$ (Eq. 28 in Reference 13, the case of large interparticle separation, since $L > R_t$) over distance d from $L-2R$ to $2D-2R$, the following expression was obtained:

$$\Delta E_{el} = \frac{\pi^2}{2}\frac{kT}{l_B}R\ln\left(\frac{2D-2R}{L-2R}\right) \quad \text{(S10)},$$

where k is Boltzmann's constant, T is the temperature, and l_B is the Bjerrum length. For DMF/water solutions at C_w of 5 and 15 vol. %, we calculated l_B to be 1.4 and 1.14 nm, respectively (*see* main text). Equation S10 uses the notations introduced in Figure S10, where R is the radius of the gold core of the NP, D is the center-to-center distance between the two neighboring PS-coated NPs and L is the center-to-center distance between the 1-st and the 3-rd PS-coated NPs (equal to $2D$ and D for θ of 180 and 60°, respectively). The variation in electrostatic energy between the 1-st and the 3-rd NPs was calculated for the range $60 \le \theta \le 300$° and plotted in Figure S9 for C_w of 5 and 15 vol. %.

The variation of the total energy of the system was deduced as

$$\Delta E_t = \Delta E_{el} + \Delta E_{st} \quad \text{(S11)}$$

and calculated separately for two cases as

$$\Delta E_t = \begin{cases} -4\pi\gamma_{PS-L}\left(R_t - \frac{L}{2}\right)R_t + \frac{\pi^2}{2}\frac{kT}{l_B}R\ln\left(\frac{2D-2R}{L-2R}\right) & \text{if} \quad L \le 2R_t \\ \frac{\pi^2}{2}\frac{kT}{l_B}R\ln\left(\frac{2D-2R}{L-2R}\right) & \text{if} \quad L > 2R_t \end{cases} \quad \text{(S12)}$$

The summary of the calculations of changes in repulsive electrostatic energy and attractive surface tension energy, as well as the change in total energy of the system, is given in Table S2 for two solvent compositions and two different angles, corresponding to the globular and chain NP configurations.

Table S2. Summary of the changes in electrostatic energy, surface tension energy and the total energy for the system containing three NPs in θ=60^o configuration.

	C_w = 5 vol. %	C_w = 15 vol. %
ΔE_{st} (kT)	-96	-69
ΔE_{el} (kT)	76	85
ΔE_t (kT)	-20	16

Figure S13 shows the variation in the total energy of the system, ΔE_t, with angle θ (defined in Figure S10) for two solvent mixtures. For C_W=5 vol.%, the deepest minimum in ΔE_t corresponded to θ=60^o (globular configuration of NPs), while for C_W=15 vol.%, the lowest minimum in ΔE_t occurred at θ=180^o (chain configuration of NPs). Both predictions were in agreement with experimental results, as shown in Fig. S6. Furthermore, in NP chains the fraction of 180 ^{o} angles (binned as 180+/-60 ^{o}) was 80%.

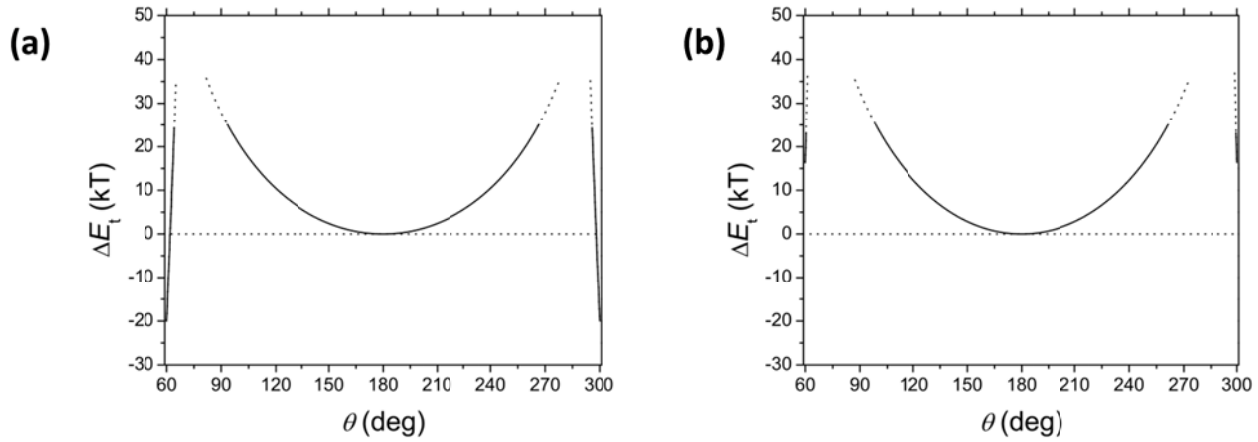

Figure S13. Variation in the total energy of interactions between two PS-coated gold NPs, plotted as a function of angle θ (as described in Figure S10 for C_W = 5 vol. % (a) and C_W = 15 vol.% (b).

References

1. Jana, N.R.; Gearheart, L.; Murphy, C.J. *Langmuir*. **2001**, *17*, 6782-6786.

2. Liu, K.; Resetco, C.; Kumacheva, E. *Nanoscale*. **2012**, *4*, 6574-6580.

3. Figuerola, A. et al. *Adv. Mater*. **2009**, *21*, 550-554.

4. Yang, M.; Chen , G.; Zhao, Y.; Silber, G.; Wang , Y.; Xing, S.; Han, Y.; Chen, H. *Phys. Chem. Chem. Phys.* **2010**, *12*, 11850-11860.

5. Sánchez-Iglesias, A. et al. *ACS Nano*. **2012**, *6*, 11059-11065.

6. Grzelczak, M.; Sánchez-Iglesias, A.; Mezerji, H.H.; Bals, S.; Pérez-Juste, J.; Liz-Marzán, L.M. *Nano Lett.*, **2012**, *12*, 4380-4384.

7. (a) Fowkes, F. M. *J. Phys. Chem*. **1962**, *66*, 382-382; (b) Li, I.T.S.; Walker, G.C. *J. Am. Chem. Soc.* **2010**, *132*, 6530–6540.

8. Israelachvili, J.N. *Intermolecular and Surface Forces*. Acad. Press: San Diego, CA, 2011.

9. Owens, D. K; Wendt, R. C. *J. Appl. Polym. Sci*. **1969**, *13*, 1741-174.

10.Wu, S. *Polymer Interface and Adhesion*. Marcel Dekker: New York, 1982.

11. Żenkiewicz, M. *J. AMME*. **2007**, *24*, 1, 137-145.

12. Ober, R.; Paz, L.; Taupin, C.; Pincus, P.; Boileau, S. *Macromolecules*. **1983**, *16*, 50-55.

13. Calculated for a mixture containing PS (36 vol. %) and DMF/water solution (64 vol. %).

14. Zhulina, E.B.; Boulakh, A.B.; Borisov, O.V. *Z. Phys. Chem*. **2012**, *226*, 625-643.

Additional references from the main text

2b. Carbone, C.; Gardonio, S.; Moras,P.; Lounis, S.; Heide, M.; Bihlmayer, G.; Atodiresei, N.; Dederichs, P.H.; Blügel, S.; Vlaic, S.; Lehnert, A.; Ouazi, S.; Rusponi, S.; Brune, H.; Honolka, J.; Enders, A.; Kern, K.; Stepanow, S.; Krull, C.; Balashov, T.; Mugarza, A.; Gambardella, P. ***Adv. Funct. Mater***. **2011**, *21*, 1212-1228.

13. Figuerola, A.; Franchini, U.R.; Fiore, A.; Mastria, R.; Falqui, A.; Bertoni, G.; Bals, S.; Van Tendeloo, G.; Kudera, S.; Cingolani, R.; Manna, L. *Adv. Mater*. **2009**, *21*, 550-554.

16. Ana Sánchez-Iglesias. A.; Grzelczak, M.; Altantzis, T.; Goris, B.; Pérez-Juste, J.; Bals, S.; Van Tendeloo, G.; Donaldson, Jr., S. H.; Chmelka, B. H., Israelachvili, J. N.; Liz-Marzán, L.M. *ACS Nano* **2012**, *6*, 11059-11065.